

Glucose-6-Phosphate-Mediated Activation of Liver Glycogen Synthase Plays a Major Role in Hepatic Glycogen Synthesis and Glucose Homeostasis

Alexander von Wilamowitz-Moellendorff, Roger W. Hunter, Mar García-Rocha, Li Kang, Iliana López-Soldado, Lousie Lantier, Kashyap Patel, Mark W. Pegg, Carles Martinez, Martin Voss, Joaquim Calbó, Patricia T.W. Cohen, David H. Wasserman, Joan J. Guinovart, Kei Sakamoto

Materials. Diaphorase was purchased from Worthington Biochemical. Collagenase A, glucose-6-phosphate and "complete" protease inhibitor cocktail were purchased from Roche Applied Science. [¹⁴C(U)]-uridine diphosphate D-glucose and [¹⁴C(U)]-D-glucose were purchased from PerkinElmer. Polyethylenimine (25-kD linear) was purchased from Polysciences Inc. Enhanced chemiluminescence (ECL) reagent was purchased from GE Healthcare. Glucokinase activator (Cpd A) was purchased from Merck. Microcystin-LR was purchased from Enzo Life Sciences. Resazurin was purchased from Life Technologies. Human insulin (Actrapid, Novo-Nordisk) and glucose (20%) for injection were obtained from Ninewells Hospital pharmacy, Dundee. All other chemicals unless specified were obtained from Sigma.

DNA constructs. Human (BC126310) and mouse (NM_145572) *GYS2* were cloned into pCMV5 using standard molecular biology techniques. Site directed mutagenesis was performed using QuikChange methodology.

Antibodies. Total ERK1/2 (#9121), Total GS (#3886), pS641 GS (#3891), pS21/9 GSK-3 α/β (#9331), PEPCK (#6924), PKB (#9272), pS473 PKB (#9271), pT308 PKB (#2965) and pT389 p70 S6 Kinase (#9234) antibodies were purchased from Cell Signaling Technology. Anti-FBP1 (sc-32430) was purchased from Santa Cruz. Anti-GAPDH was purchased from Sigma (G8795) and Ambion (6C5). Anti-GSK3 α/β (44-610) was purchased from Life Technologies. Anti-Green fluorescent protein (GFP) was from Immunokontakt. Anti-GBE1 (AP9506c) was purchased from Abgent. Antibodies against pS641/645 GS, pS15 GP, total GP, GST and PKB α have been described previously (Bouskila et al., 2010). PKB β antibody was generated as previously described (Wullschleger et al., 2011). Total *GYS2* antibody and pS8 *GYS2* antibody was generated as previously described (Bouskila et al., 2010; Garcia-Rocha et al., 2001; Ros et al., 2009). AGL, glycogenin and STBD1 antibodies were provided by David Stapleton (University of Melbourne). Anti-GLUT2 was donated by Bernard Thorens (University of Lausanne). Anti-GK was given by Mark Magnuson (Vanderbilt University). Anti-GKR was provided by Masakazu Shiota (Vanderbilt University). Anti-G6PC was provided by Calum Sutherland (University of Dundee). Secondary antibodies were obtained from Jackson ImmunoResearch Laboratories or LI-COR.

Protein sequence. All sequence alignments were generated using Jalview 2.4 developed by the Geoff Barton Group (University of Dundee). The ClustalW Multiple sequence alignment algorithm was used for the alignment. Protein sequences listed in Fig 1A were obtained from the Swiss-Prot database. *GYS1* (*Homo sapiens*, P12807), *GYS2* (*Homo sapiens*, P54840), *GYS1* (*Mus musculus*, Q9Z1E4) *GYS2* (*Mus musculus*, Q8VCB3), *GYS2* (*Xenopus tropicalis*, Q5FVV6), *GYS2* (*Danio rerio*, Q5RGX8) and *Gsy2p* (*Saccharomyces cerevisiae*, P27472).

Preparation of tissue lysates. Frozen liver samples were homogenised using a rotor-stator homogenizer (Polytron, Kinematica AG) in 20 volumes of ice-cold lysis buffer, clarified for 5min at 3,000 \times g at 4°C and protein concentration determined using BCA reagent (Pierce) with BSA as standard. Lysates were stored at -80°C.

SUPPLEMENTARY DATA

Western blotting. Tissue lysates (20-30µg) were denatured in Laemmli buffer, separated by SDS-PAGE and transferred to nitrocellulose. Membranes were blocked in 50mM Tris-HCl pH 7.6, 137mM NaCl and 0.1% (v/v) Tween-20 (TBST) containing 10% (w/v) skimmed milk or 5% (w/v) BSA for 1h at RT and incubated overnight at 4°C with the indicated primary antibodies. Detection was performed using horseradish peroxidase conjugated secondary antibodies and enhanced chemiluminescence reagent or by fluorescence using a LI-COR Odyssey infrared detection system according to the manufactures instructions.

PKB activity assays. PKBβ was immunoprecipitated from liver extracts (0.5mg) and phosphotransferase activity (expressed in mU/mg, 1U=1nmol.min⁻¹) measured using Crosstide as previously described (McManus et al., 2005).

Tissue metabolites. Frozen liver samples were crushed in a liquid nitrogen cooled mortar and homogenised in 0.6M HClO₄, 1mM EDTA. Extracts were clarified at 10,000 g for 10min at 4°C and neutralised with 2M KOH, 0.4M imidazole. G6P was measured using a coupled fluorimetric assay containing 50mM triethanolamine pH 7.6, 1 mM MgCl₂, 50µM NAD⁺, 0.05U/ml glucose-6-phosphate dehydrogenase, 0.1U/ml diaphorase and 8µM resazurin (purified by TLC) using a Molecular Devices Gemini EM fluorescence microplate reader (EX/EM 550/590nm). UDP-glucose was measured by oxidation with 0.008U/ml UDP-glucose dehydrogenase in 50mM Tris pH 8.1, 2mM MgCl₂ and 100µM NAD⁺ for 30min. NADH was subsequently detected using the resazurin/diaphorase system as described for G6P. Glycogen was assayed in KOH-digested tissues as previously described (Bouskila et al., 2008; McManus et al., 2005). Total lipid was extracted using the method of Folch (Folch et al., 1957) and triglyceride assayed using a commercial kit (Sigma TR0100).

Blood metabolites. Blood glucose levels were monitored from tail vein blood using the AlphaTRAK Blood Glucose Monitoring System (Abbott). Plasma insulin levels were determined using a commercial ELISA (Millipore). Plasma lactate was measured enzymatically using reagents from BioVision.

Glucose tolerance test (GTT). After overnight or short term (6h) fasting, glucose (2mg/g body mass) was administered intraperitoneally and blood glucose monitored by tail bleeding using a glucometer over a 2h period.

mRNA extraction and qPCR. Total RNA was isolated from liver using RNeasy mini kits (Qiagen) and cDNA synthesised using iScript cDNA Synthesis Kit (BioRad). qPCR was performed using SsoFast EvaGreen Supermix (BioRad) in 20µl reactions containing 15 ng cDNA and 400nM primers in a CFX-96 thermal cycler (BioRad). Relative mRNA levels were calculated using delta-delta C_t (Yuan et al., 2006) and normalized using *Actb* and *Hprt1*. Sense and antisense primers: *Actb* (5'-CAACGAGCGGTTCCGATG-3', 5'-GCCACAGGATTCCATACCCA-3'), *Hprt1* (5'-CCAGCGTCGTGATTAGCGATGATG-3', 5'-GAGCACACAGAGGGCCACAAT G-3'), *Gys2* (5'-GGCCTCCCTGGGTGTGTTCTTC-3', 5'-GAAGCTGGGGGCAGGACGAAGC-3') *Gys1* (5'-GGATGTTGCAGCCTCAGCTT-3', 5'-GATGTTGCAGGTGTCCCAAAG-3').

SUPPLEMENTARY DATA

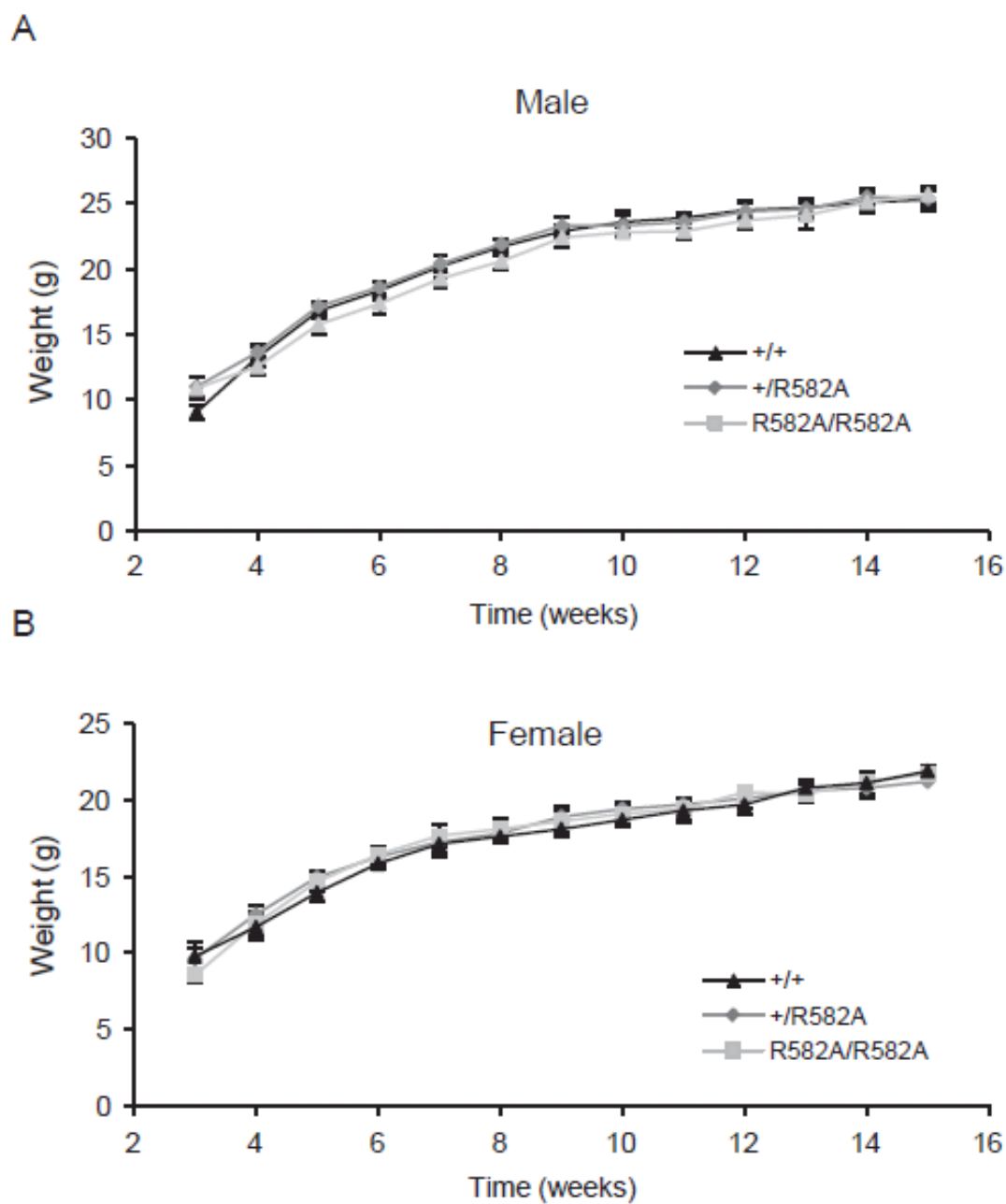
Adenovirus. Recombinant adenoviruses coding for GFP (Ad-GFP) (Gomis et al., 2002) and PTG fused to GFP (Ad-PTG) (Vilchez et al., 2007) have been described. Adenovirus coding for wild-type and R582A mouse GYS2 were generated using the ViraPower system from Life Technologies and packaged using HEK293A cells. MOI of 8 was used for GYS2 WT, GFP and GFP-PTG and MOI of 16 was used for GYS2 R582A for infection.

Immunofluorescence. Hepatocytes seeded on collagen-coated glass coverslips (10mm × 10 mm) were fixed in PBS containing 4% (w/v) paraformaldehyde. Localization of overexpressed GYS2 was studied using anti-liver glycogen synthase L1 (Garcia-Rocha et al., 2001) and Texas Red-conjugated donkey anti-rabbit IgG (Jackson ImmunoResearch). For GFP and PTG overexpression, the auto fluorescence from GFP was used. Nuclei were stained with Hoechst 33342 (Life Technologies). Confocal images were taken with a Leica SP2 microscope using a ×63 objective without confocal magnification.

Euglycaemic-hyperinsulinaemic clamp. All procedures required for the hyperinsulinaemic–euglycaemic clamp were approved by the Vanderbilt University Animal Care and Use Committee. Catheters were implanted into a carotid artery and a jugular vein of mice for sampling and infusions respectively five days before the study as described by Berglund et al. (Berglund et al., 2008). Insulin clamps were performed on mice fasted for 5h using a modification of the method described by Ayala et al. (Ayala et al., 2006). [3-³H]-glucose was primed (2.4μCi) and continuously infused for a 90min equilibration and basal sampling periods (0.04μCi/min). [3-³H]-glucose was mixed with the non-radioactive glucose infusate (infusate specific activity of 0.4 μCi/mg) during the 2 h clamp period. Arterial glucose was clamped using a variable rate of glucose (plus trace [3-³H]-glucose) infusion, which was adjusted based on the measurement of blood glucose at 10 min intervals. By mixing radioactive glucose with the non-radioactive glucose infused during a clamp, deviations in arterial glucose specific activity are minimized creating steady state conditions. The calculation of glucose kinetics is therefore more robust (Finegood et al., 1987). Baseline blood or plasma variables were calculated as the mean of values obtained in blood samples collected at -15 and -5min. At time zero, insulin infusion (2.5mU/kg of body weight per min) was started and continued for 120min. Mice received heparinized saline-washed erythrocytes from donors at 5μl/min to prevent a fall in haematocrit. Insulin clamps were validated by assessment of blood glucose over time. Blood was taken at 80-120min for the determination of D-[3-³H]-glucose. Clamp insulin was determined at *t*=100 and 120min. After the last sample, mice were anaesthetized and liver tissue was freeze-clamped for biochemical analysis. Plasma insulin was determined by ELISA. Radioactivity of [3-³H]-glucose in plasma samples were determined by liquid-scintillation counting. Glucose appearance and disappearance rates were determined using non-steady-state equations (Steele et al., 1956). Endogenous glucose production was determined by subtracting the GIR (glucose infusion rate) from the total glucose production. The glucose metabolic clearance was calculated by dividing glucose disappearance by arterial glucose concentration.

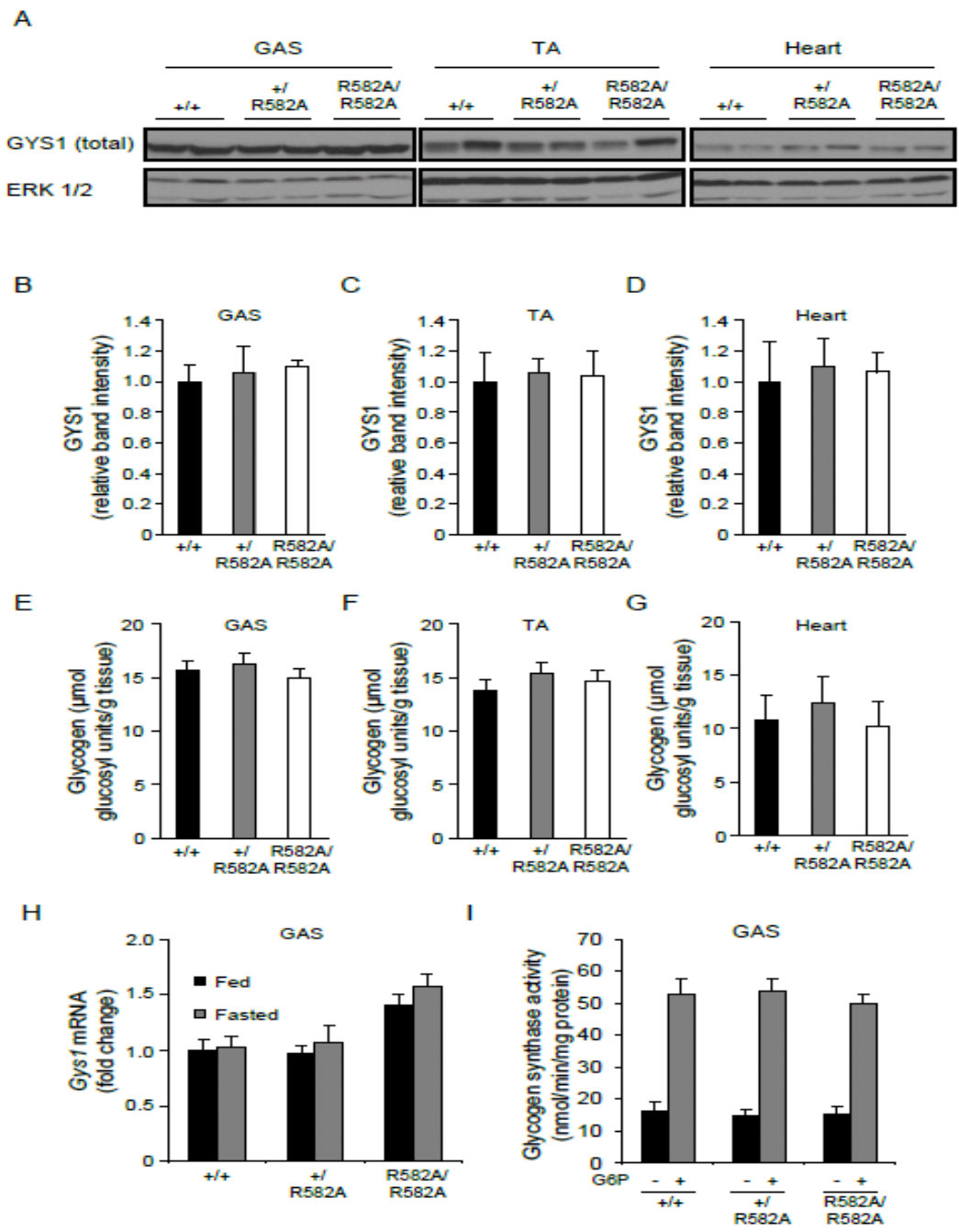
SUPPLEMENTARY DATA

Supplementary Figure 1. Growth curve of male and female $GYS2^{+/+}$, $GYS2^{+/R582A}$ and $GYS2^{R582A/R582A}$ mice. Male (A) and female (B) mice were weighed weekly between 9 and 11 am for 12 weeks, starting at 3 weeks of age (n=8-16/group).



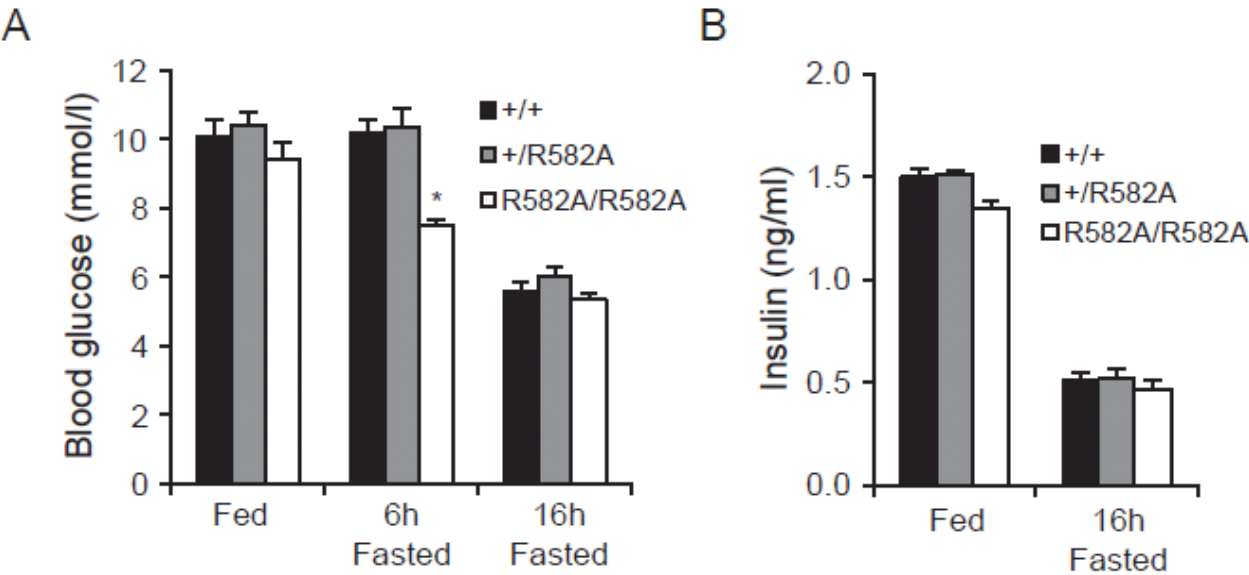
SUPPLEMENTARY DATA

Supplementary Figure 2. GYS1 expression, glycogen levels, *Gys1* mRNA and GYS1 activity in skeletal muscle and heart from GYS2^{+/+}, GYS2^{+/^{R582A}} and GYS2^{R582A/R582A} mice. (A) Lysates from GAS and TA muscle and heart from *ad libitum* fed mice were immunoblotted using the indicated antibodies. ERK1/2 was used as a loading control. (B-D) GYS1 protein levels were quantified by immunoblotting using a LI-COR Odyssey infrared imaging system (normalized to GAPDH) in GAS (B), TA (C) and heart (D) (n=4/group). (E-G) Tissue glycogen in GAS (E), TA (F) and heart (G) (n=4-6/group). (H) Total RNA was isolated from GAS of *ad libitum* fed and overnight fasted mice and *Gys1* mRNA levels quantified using qPCR. Data was normalized to *Gys1* mRNA levels in fed GYS2^{+/+} mice (n=6/group). (I) GS activity in *ad libitum* fed GAS lysates was measured in the presence or absence of G6P (10mM) (n=6/group).

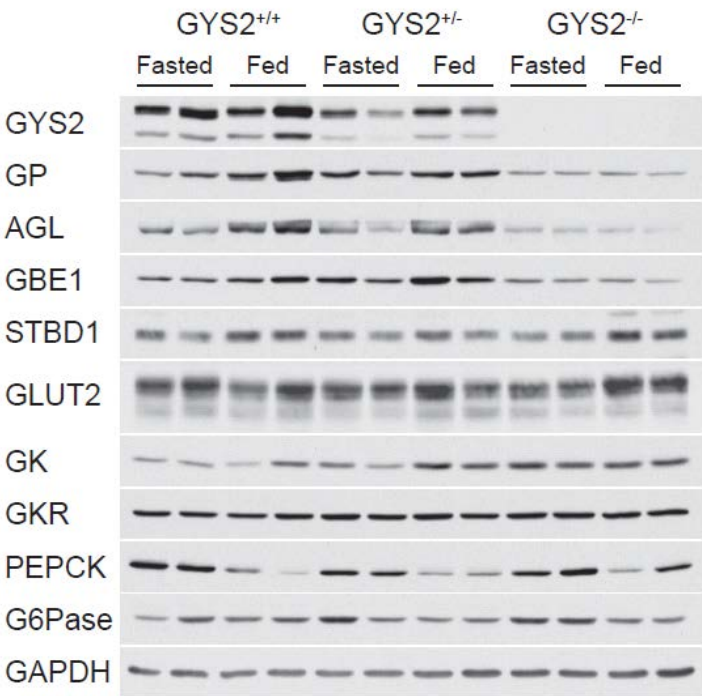


SUPPLEMENTARY DATA

Supplementary Figure 3. Blood glucose and plasma insulin levels in GYS2^{+/+}, GYS2^{+R582A} and GYS2^{R582A/R582A} mice. (A) Blood glucose levels were measured in *ad libitum* fed or fasted (6 or 16h) GYS2^{+/+}, GYS2^{+R582A} and GYS2^{R582A/R582A} mice using a glucometer. * p < 0.05 GYS2^{+/+} versus other genotypes (n=16-22/group). (B) Plasma insulin levels were measured from tail vein blood from *ad libitum* fed and 16h fasted GYS2^{+/+}, GYS2^{+R582A} and GYS2^{R582A/R582A} mice (n=7-10/group).



Supplementary Figure 4. Hepatic glycogen-associated proteins are down-regulated in livers from GYS2-null mice. Livers from overnight fasted or randomly fed GYS2^{+/+}, GYS2^{+/-} and GYS2^{-/-} mice were homogenised and analyzed for expression of key enzymes involved in glucose metabolism and glycogen-associated proteins by immunoblotting with the indicated antibodies (n=2/group).

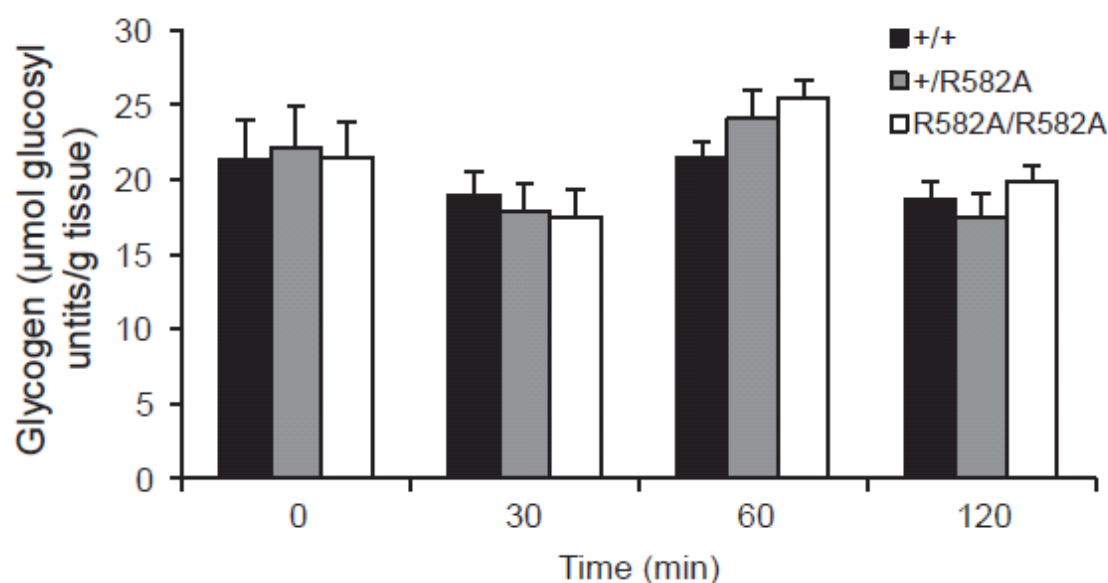


SUPPLEMENTARY DATA

Supplementary Figure 5. Adenoviral overexpression of GYS2 mutants in GYS2^{-/-} hepatocytes has no effect on GK expression. Primary hepatocytes from GYS2^{-/-} mice were infected with adenovirus expressing GYS2 WT, GYS2 R582A and GYS2 E510A as described in Fig. 2. The resulting extracts were analyzed for expression of GYS2 and GK by immunoblotting (GAPDH is included as a loading control). Results are representative of two independent experiments.

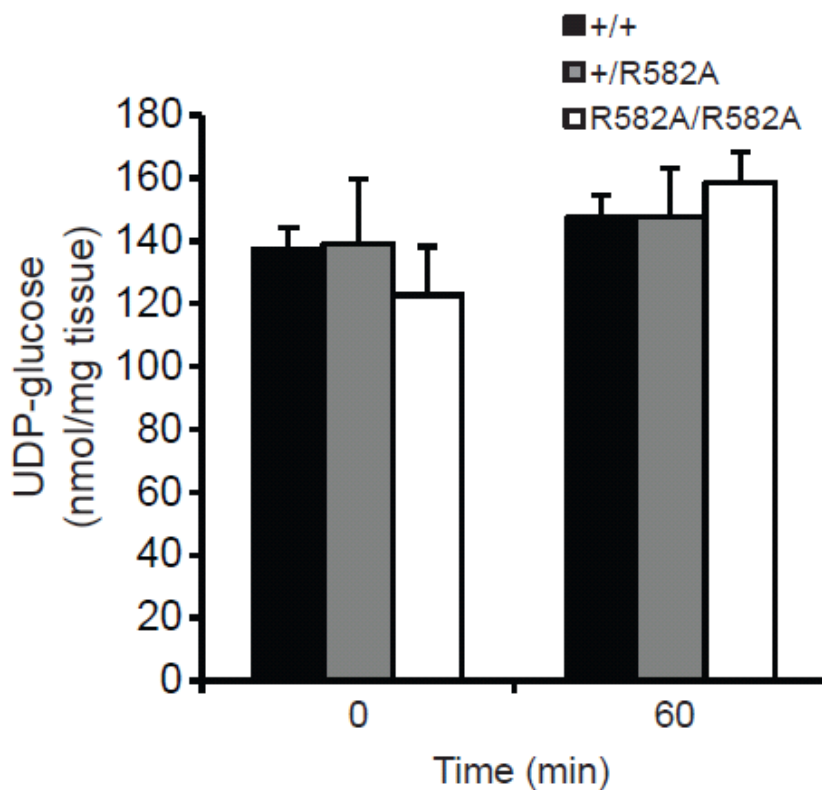


Supplementary Figure 6. GAS glycogen levels after bolus glucose injection in GYS2^{+/+}, GYS2^{+/R582A} and GYS2^{R582A/R582A} mice. GYS2^{+/+}, GYS2^{+/R582A} and GYS2^{R582A/R582A} mice were fasted for 16h, followed by intraperitoneal administration of glucose (2mg/g body weight). Mice were sacrificed at the indicated time points and glycogen levels determined in GAS (n=3-6/group).



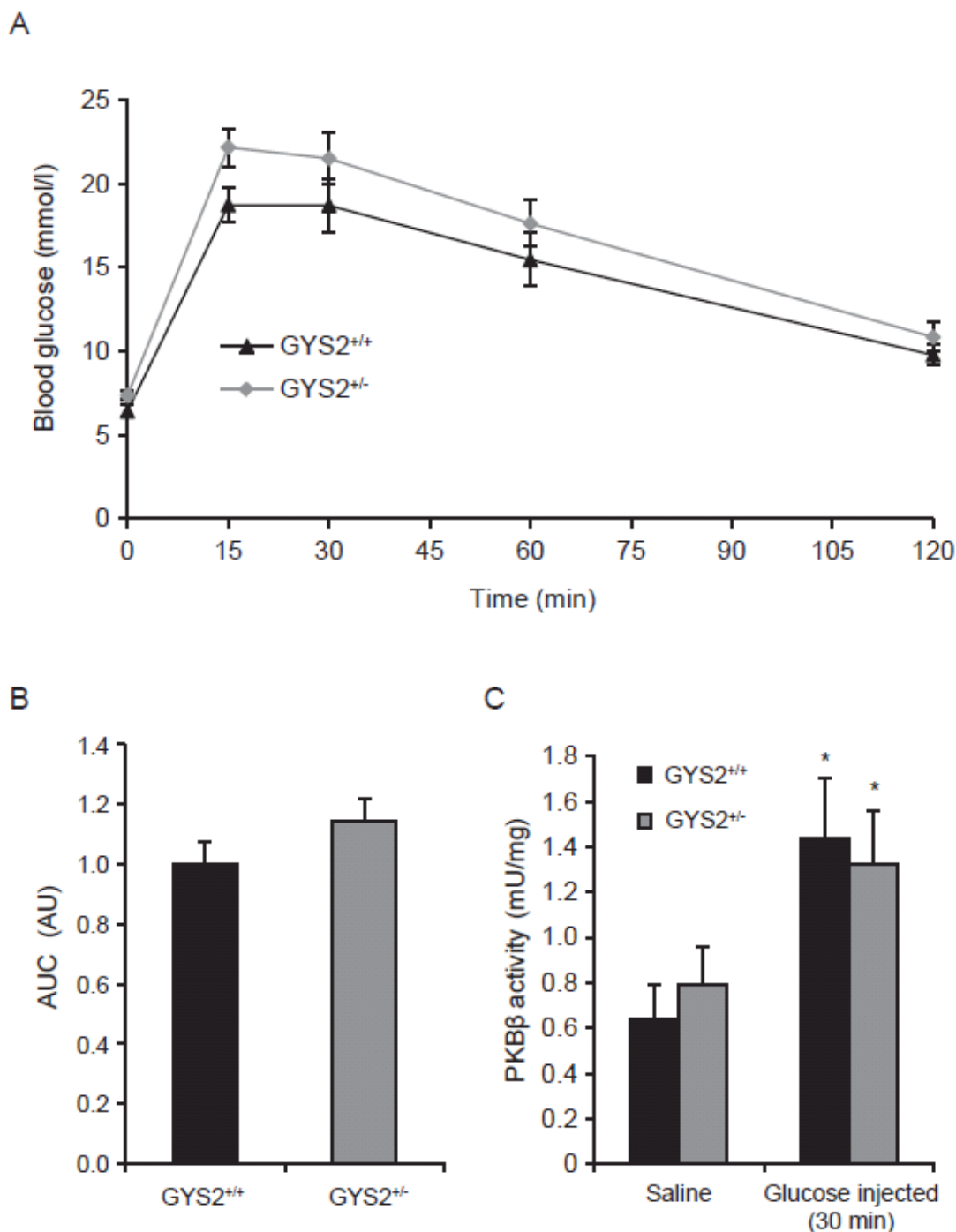
SUPPLEMENTARY DATA

Supplementary Figure 7. Hepatic UDP-glucose levels in response to i.p. glucose administration in GYS2^{+/+}, GYS2^{+/R582A} and GYS2^{R582A/R582A} mice. Overnight fasted mice were sacrificed before (0min) or after (60min) an i.p. glucose bolus (2mg/g body weight). UDP-glucose was measured in extracts from freeze-clamped livers as described in the methods. Results are expressed as mean \pm SEM (n=3-6/group).



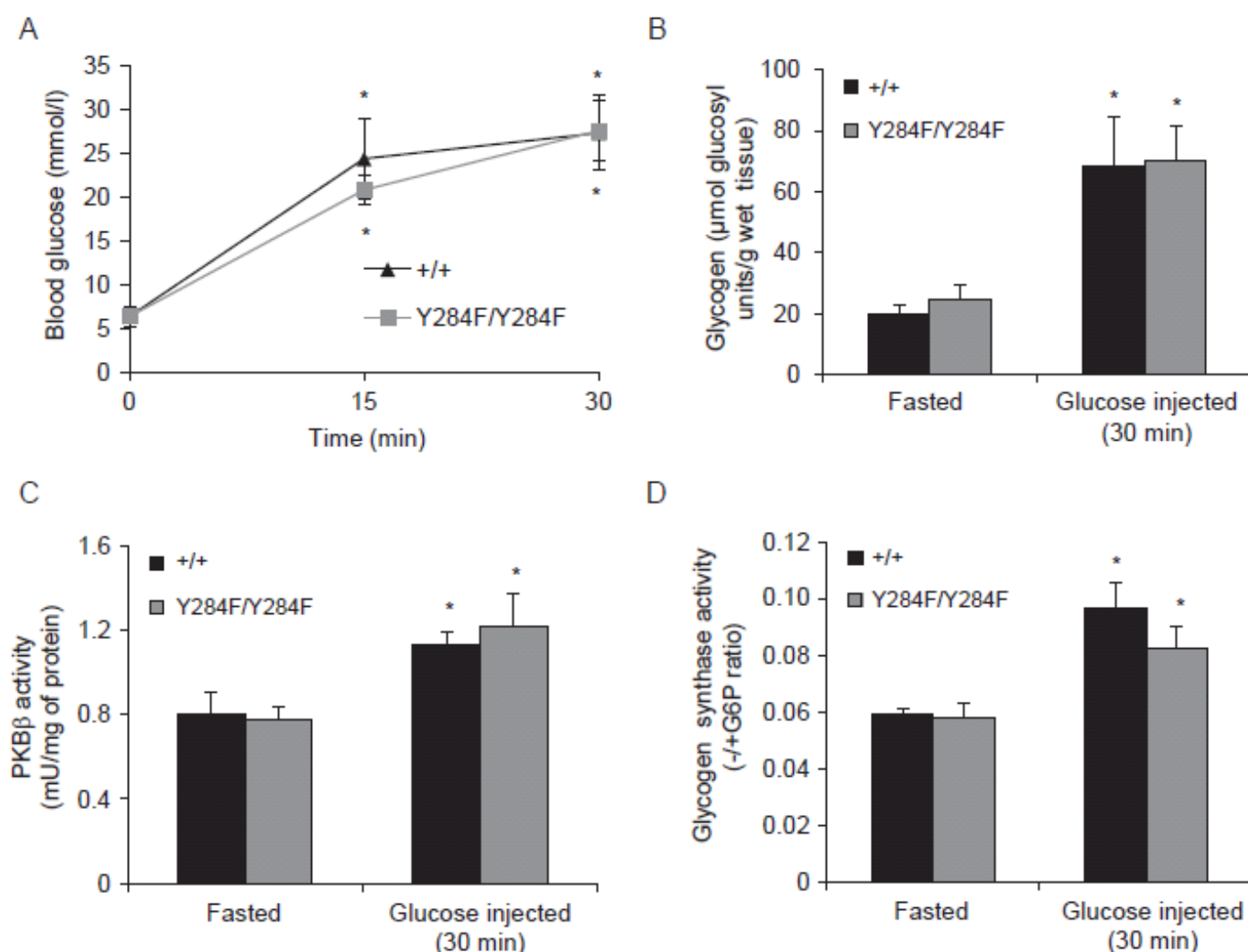
SUPPLEMENTARY DATA

Supplementary Figure 8. Blood glucose and PKB β activity in GYS2^{-/+} mice after bolus glucose injection. (A-B) GYS2^{-/+} and GYS2^{+/+} mice were fasted for 16h followed by intraperitoneal administration of glucose (2mg/g body weight). (A) Blood glucose levels were measured at the indicated time points post-injection by tail bleeding. (B) Area under the curve (AUC) for the data in (A) was calculated using 16h fasting blood glucose levels as baseline. Results are expressed in arbitrary units (AU) (n=5-7/group). (C) GYS2^{-/+} and GYS2^{+/+} mice were fasted for 16h followed by intraperitoneal administration of glucose (2mg/g body weight) or saline. After 30min, mice were sacrificed and liver samples taken for determination of PKB β kinase activity in immunoprecipitates *p<0.05 GYS2^{+/+} versus other genotypes (n=5-7/group).



SUPPLEMENTARY DATA

Supplementary Figure 9. Blood glucose levels, liver glycogen levels and PKB β and GS activity in GL^{Y284F/Y284F} and GL^{+/+} mice after glucose bolus injection. (A-D) GL^{Y284F/Y284F} and GL^{+/+} male mice were fasted for 16h followed by intraperitoneal administration of glucose (2 mg/g body weight) or saline. * $p < 0.05$ fasted versus glucose injected ($n = 5-7$ /group). (A) Blood glucose levels were measured at the indicated time points post-injection by tail bleeding. (B-D) Mice were sacrificed after 30min and analyzed as follows. (B) Liver glycogen levels. (C) PKB β was immunoprecipitated from liver lysates and assayed for phosphotransferase activity. (D) GS activity was measured in liver lysates in the presence and absence of 10mM G6P. Results are expressed as the activity ratio (-/+G6P). Note that the inhibition of PP1-G_L by GP α is a mechanism operating a switch from glycogen synthesis to glycogen breakdown during short-term fasting and would not be expected to operate after a 16-h fast (Kelsall et al., 2009). During long-term fasting, the levels of G_L and PTG/R5 decrease (Browne et al., 2001) and regulate the glycogen-bound PP1 phosphatase activity and thus the activation of GS in WT and GL^{Y284F/Y284F} mice.



References

- Ayala, J.E., Bracy, D.P., McGuinness, O.P., and Wasserman, D.H. (2006). Considerations in the design of hyperinsulinemic-euglycemic clamps in the conscious mouse. *Diabetes* 55, 390-397.
- Berglund, E.D., Li, C.Y., Poffenberger, G., Ayala, J.E., Fueger, P.T., Willis, S.E., Jewell, M.M., Powers, A.C., and Wasserman, D.H. (2008). Glucose metabolism in vivo in four commonly used inbred mouse strains. *Diabetes* 57, 1790-1799.
- Bouskila, M., Hirshman, M.F., Jensen, J., Goodyear, L.J., and Sakamoto, K. (2008). Insulin promotes glycogen synthesis in the absence of GSK3 phosphorylation in skeletal muscle. *Am J Physiol Endocrinol Metab* 294, E28-35.
- Bouskila, M., Hunter, R.W., Ibrahim, A.F., Delattre, L., Pegg, M., van Diepen, J.A., Voshol, P.J., Jensen, J., and Sakamoto, K. (2010). Allosteric regulation of glycogen synthase controls glycogen synthesis in muscle. *Cell Metab* 12, 456-466.
- Browne, G.J., Delibegovic, M., Keppens, S., Stalmans, W., and Cohen, P.T. (2001). The level of the glycogen targeting regulatory subunit R5 of protein phosphatase 1 is decreased in the livers of insulin-dependent diabetic rats and starved rats. *Biochem J* 360, 449-459.
- Finegood, D.T., Bergman, R.N., and Vranic, M. (1987). Estimation of endogenous glucose production during hyperinsulinemic-euglycemic glucose clamps. Comparison of unlabeled and labeled exogenous glucose infusates. *Diabetes* 36, 914-924.
- Folch, J., Lees, M., and Sloane Stanley, G.H. (1957). A simple method for the isolation and purification of total lipides from animal tissues. *J Biol Chem* 226, 497-509.
- Garcia-Rocha, M., Roca, A., De La Iglesia, N., Baba, O., Fernandez-Novell, J.M., Ferrer, J.C., and Guinovart, J.J. (2001). Intracellular distribution of glycogen synthase and glycogen in primary cultured rat hepatocytes. *Biochem J* 357, 17-24.
- Gomis, R.R., Cid, E., Garcia-Rocha, M., Ferrer, J.C., and Guinovart, J.J. (2002). Liver glycogen synthase but not the muscle isoform differentiates between glucose 6-phosphate produced by glucokinase or hexokinase. *J Biol Chem* 277, 23246-23252.
- Kelsall, I.R., Rosenzweig, D., and Cohen, P.T. (2009). Disruption of the allosteric phosphorylase a regulation of the hepatic glycogen-targeted protein phosphatase 1 improves glucose tolerance in vivo. *Cell Signal* 21, 1123-1134.
- McManus, E.J., Sakamoto, K., Armit, L.J., Ronaldson, L., Shpiro, N., Marquez, R., and Alessi, D.R. (2005). Role that phosphorylation of GSK3 plays in insulin and Wnt signalling defined by knockin analysis. *EMBO J* 24, 1571-1583.
- Ros, S., Garcia-Rocha, M., Dominguez, J., Ferrer, J.C., and Guinovart, J.J. (2009). Control of liver glycogen synthase activity and intracellular distribution by phosphorylation. *J Biol Chem* 284, 6370-6378.
- Steele, R., Wall, J.S., De Bodo, R.C., and Altszuler, N. (1956). Measurement of size and turnover rate of body glucose pool by the isotope dilution method. *Am J Physiol* 187, 15-24.
- Vilchez, D., Ros, S., Cifuentes, D., Pujadas, L., Valles, J., Garcia-Fojeda, B., Criado-Garcia, O., Fernandez-Sanchez, E., Medrano-Fernandez, I., Dominguez, J., et al. (2007). Mechanism suppressing glycogen synthesis in neurons and its demise in progressive myoclonus epilepsy. *Nat Neurosci* 10, 1407-1413.
- Wullschlegel, S., Sakamoto, K., Johnstone, L., Duce, S., Fleming, S., and Alessi, D.R. (2011). How moderate changes in Akt T-loop phosphorylation impact on tumorigenesis and insulin resistance. *Dis Model Mech* 4, 95-103.
- Yuan, J.S., Reed, A., Chen, F., and Stewart, C.N., Jr. (2006). Statistical analysis of real-time PCR data. *BMC Bioinformatics* 7, 85.